Energies and lifetimes of excited states in copperlike Kr VIII

A. E. Livingston,* L. J. Curtis,† R. M. Schectman,† and H. G. Berry
Physics Division, Argonne National Laboratory, Argonne, Illinois 60439
(Received 8 March 1979)

The spectrum of Kr VIII has been observed between 180 and 2000 Å by using foil excitation of 2.5–3.5-MeV krypton ions. Twenty new transitions have been classified and eleven new excited-state energies have been determined within the $n = 4$–7 shells. The ionization potential is derived to be 1015800 ± 200 cm^{-1}. The excited-state energies and fine structures are compared with recent relativistic Hartree-Fock calculations. The $4p$-state lifetime has been measured by performing a simultaneous analysis of decay data for the $4p$ level and for its dominant cascade-repopulating levels. The $4p$ lifetime is found to be 30% shorter than previously measured values and is in excellent agreement with the result of a recent multiconfiguration Hartree-Fock calculation. The source of the discrepancy between this result and earlier measurements is discussed.

I. INTRODUCTION

The experimental determination of the atomic structures and excited-state lifetimes in highly stripped alkalilike ions is important in modeling and diagnostic studies of both laboratory and astrophysical plasmas as well as for detailed testing of current relativistic atomic calculations. Ions of the Cu I isoelectronic sequence are prominent as impurities in high-temperature magnetically confined plasmas[1] and the emission spectra are also observed in spark sources,[2-6] in laser-produced plasmas,[6,7] and with beam-foil excitation.[8-12] However, the atomic structures of moderately ionized copperlike systems are scarcely known. The alkalilike character of these spectroscopically important ions suggests that fairly reliable calculations of both the atomic structures and lifetimes should be possible, and several such theoretical studies have been reported recently.[13-18]

For copperlike Kr VIII, transition wavelengths for the $4s$-$4p$ resonance multiplet have been measured by Fawcett *et al.*[19] in a high-temperature (ζ) plasma. Tentative identifications for the $4p$-$4d$ transition wavelengths were reported in a recent beam-foil study by Druetta and Buchet,[10] although no indication of the associated wavelength precision was given. No other excited states in Kr VIII have been classified previously, although an extensive wavelength list for foil-excited krypton spectra has been compiled by Cardon.[20] Precise wavelength measurements involving more highly excited states in Kr VIII are needed in order to provide atomic structure data for testing the accuracies of current relativistic calculations in the regime of moderately high ionicity for copperlike systems.

Lifetime measurements for the $4p$ state in Kr VIII have been performed previously by several groups using beam-foil excitation.[10-12] However, these measurements are all in serious disagreement with theoretical calculations carried out using various methods.[13-18] Similar discrepancies between theory and experiment exist for the lifetimes of low-lying excited states in other ionized members of the Cu I and Na I isoelectronic sequences. It has been pointed out by Crossley *et al.*[21] and by Younger and Wiese[22] that such $\Delta n = 0$ transitions involve an unusually difficult experimental situation for which the excited states are heavily repopulated by cascades from highly excited high-l states, including some with lifetimes comparable to that of the level being studied, as well as from other low-lying states. For these reasons, a careful remeasurement of the $4p$ lifetime in Kr VIII is clearly needed, with special attention being devoted to the effects of cascade contributions.

In this paper we present new wavelength classifications involving $n = 4, 5, 6$, and 7 states in Kr VIII, based upon our observations of the beam-foil spectrum of krypton. The excited-state energies that are derived from these wavelengths allow detailed comparison to be made with current relativistic atomic structure calculations for this region of the Cu I isoelectronic sequence. Using these newly identified transitions we have been able to perform the first direct measurements of the decay characteristics of states that repopulate this $4p$ level by cascade feeding. We have utilized methods involving the simultaneous treatment of correlated-decay data in order to extract the $4p$ lifetime from measured decays for the $4p$ state and cascading states. We have also analyzed the $4p$-state decay data, using multiexponential-fitting techniques, to show how even this approach can be made more reliable. Our results are compared with the previously measured lifetimes and with current theoretical calculations.

 © 1980 The American Physical Society

II. JOINT ANALYSIS OF CASCADE-RELATED DECAY CURVES

The measured decay curve[23] of the $4p$ level, $I_{4p}(t)$, is related to its direct cascades from the ns and nd levels, $I_{ns}(t)$ and $I_{nd}(t)$, by the instantaneous population equation

$$\frac{dI_{4p}}{dt} = \xi_{4d} I_{4d}(t) + \sum_{n=5}^{\infty} [\xi_{nd} I_{nd}(t) + \xi_{ns} I_{ns}(t)] - \alpha_{4p} I_{4p}(t) , \quad (1)$$

where ξ_{nl} denotes a normalizing constant which, if known, would convert the arbitrary units of the various decay curves to a common scale, and $\alpha_{4p} = 1/\tau_{4p}$ is the reciprocal mean life of the $4p$ level. Equation (1) can be rewritten in the form

$$y = \alpha_{4p} - \xi_{4d}(x + x_0) , \quad (2)$$

where

$$y \equiv -d(\ln I_{4p})/dt , \quad (3)$$

$$x \equiv I_{4d}(t)/I_{4p}(t) , \quad (4)$$

$$x_0 \equiv \sum_{n=5}^{\infty} \frac{[\xi_{nd} I_{nd}(t) + \xi_{ns} I_{ns}(t)]}{\xi_{4d} I_{4p}(t)} . \quad (5)$$

Written in this fashion, y contains all information concerning the primary decay curve, x contains all information concerning all of the yrast ($l = n - 1$) cascades, and x_0 contains all information concerning all of the nonyrast cascades. In a case where the dominant cascade repopulation is from the yrast chain, Eq. (2) becomes

$$y \cong \alpha_{4p} - \xi_{4d} x . \quad (6)$$

The reciprocal mean life and normalizing constant can be obtained from the intercept and slope of a y vs x plot, with y and x computed regionwise from the measured I_{4p} and I_{4d}. Neglecting cascades outside the yrast chain, we express the initial replenishment ratio[23] $R(0)$ in terms of the fitting parameters by

$$R(0) = \xi_{4d} I_{4d}(0)/\alpha_{4p} I_{4p}(0) . \quad (7)$$

The largest contribution to x_0 would be expected to arise from the $4p$-$5d$ transition. As will be discussed in Sec. V, there is a fortuitous cancellation in the $4p$-$5d$ transition integral for Kr VIII, causing it to branch nearly 100% to the $5p$-$5d$ and $4f$-$5d$ channels. Cascading from the $5s$ state was found to have little influence on the analysis, as will be discussed later. This situation makes Kr VIII uniquely well suited among members of the Cu I isoelectronic sequence for analysis by this method.

III. EXPERIMENT

The Dynamitron accelerator at Argonne National Laboratory provided beam currents of up to several μA of Kr^+ ions in the energy range 2.5–3.5 MeV. The ions were excited by passage through 5-μg/cm^2 carbon foils, which introduced an energy loss[24] of about 2%, yielding a post-foil ion velocity for 3.5-MeV incident ions of 2.81 mm/ns. The emission from excited krypton ions was dispersed by using either a McPherson 2.2-m grazing-incidence monochromator or a McPherson 1-m normal-incidence monochromator. Photons were detected with a windowless Channeltron electron multiplier or an EMR 541F multiplier phototube (LiF window), in conjunction with standard pulse-counting electronics.

Spectra were recorded by scanning the detector along the Rowland circle with a synchronous motor for the grazing-incidence monochromator, and by advancing the grating drive with a stepping motor for the normal-incidence monochromator. The wavelength range 100–2500 Å was surveyed in this manner.

The first-order linewidths were less than 1 Å for all spectra recorded. For the normal-incidence work, this required refocusing[25] of the monochromator to eliminate the first-order Doppler broadening that results from observing the moving source with an instrument having a large acceptance angle. Emission line centers could be located usually to within ±0.1 Å by means of computer fitting and reference to wavelength standards. Above 400 Å, Kr VI and VII lines were available as standards. Additional standards were obtained by using a foil-excited He^+ beam to produce the He II Lyman series, and foil excitation of O^+ ions to produce the vacuum-ultraviolet standard lines of Edlén.[26] Both the first and second orders of dispersion were employed to study the spectra.

For lifetime measurements, the grazing-incidence monochromator was used, with a modified entrance slit[27] placed close to the beam for much-improved spatial resolution. The resultant "time window" along the beam that was accepted by the monochromator was about 30 ps. Photons representing a chosen transition were collected at various distances from the foil for counting periods determined by the collection of a fixed amount of ion charge in a Faraday cup. The spatial separation of data points along the beam was about 30 μ (~20 ps) for the more rapid portions of the decays near the foil, with wider intervals being used in the decay tails. The decays were studied over a distance corresponding to about 5 ns, or some twenty $4p$ lifetimes. The detector dark count was below one per minute and was negligible compared with the signal over most of the decay lengths. Decay data were obtained by advancing the foil along the beam using a stepping motor. The control of stepping motors and the acquisition

and storage of data were accomplished by an on-line PDP 11/45 computer.

IV. RESULTS

A. Spectra

We have classified 25 transitions in the level scheme of KrVIII from the beam-foil spectra (see Table I). Twenty of these lines represent new classifications. Also listed in Table I are the theoretical wavelengths provided by relativistic Hartree-Fock calculations of Cheng and Kim.[16] In Table II we tabulate the excited-state energies derived from our wavelength observations (the $4p$ levels are based upon the more precise wavelengths for the resonance doublet reported previously by Fawcett *et al.*[19]). An energy-level diagram summarizing these results is shown in Fig. 1.

Examples of sections of our beam-foil spectra are given in Figs. 2 and 3. In Fig. 2 are shown the well-resolved fine-structure components of the $4p$-$4d$ multiplet at 434.1, 450.7, and 453.3 Å. The nearby line[28] at 445.33 Å has been classified recently[10,29] as the $4s4p\,^3P_2$-$4s4d\,^3D_3$ transition in KrVII and may be used as a reference wavelength for these KrVIII lines. We note that the $^3P_1$-$^3D_2$ component of this KrVII multiplet lies[28,29] at 434.28 Å and is not resolved from the KrVIII $4p_{1/2}$-$4d_{3/2}$ line at 434.1 Å. This blending has been taken into account in the determination of the KrVIII wavelength by assuming that the line intensities within each multiplet are those predicted for LS-coupling conditions.

The $4f$-$5g$ transition is expected to lie in a relatively complicated region of the beam-foil spectrum near the KrVII $4s^2\,^1S$-$4s4p\,^1P$ resonance line at 585.37 Å. We have classified the feature observed at 583.2 Å as the $4f$-$5g$ transition in KrVIII. In Fig. 3 this line is clearly stronger with respect to the KrVII transition at 3.6 MeV than at 2.5 MeV and follows the intensity of $5g$-$6h$ transition at 1157.2 Å that we have also classified in KrVIII. Furthermore, in Fig. 3b, 583.2 Å is seen to be broader than the KrVII line, reflecting the unresolved fine-structure interval that is expected to be about 0.2 Å (see note added in proof).

The observations of resolved fine-structure

TABLE I. Wavelength observations in Kr VIII.

Transition	Wavelength (Å) This work	Other experiments	Theory [a]		
$4s_{1/2}$-$5p_{3/2}$	181.5 ± 0.2		183.7		
$4s_{1/2}$-$5p_{1/2}$	182.8 ± 0.2		185.0		
$4d_{3/2}$-$5f_{5/2}$	285.0 ± 0.2		288.0		
$4d_{5/2}$-$5f_{5/2,7/2}$	286.2 ± 0.2		289.1		
$4p_{1/2}$-$5s_{1/2}$	288.5 ± 0.3		292.7		
$4p_{3/2}$-$5s_{1/2}$	297.1 ± 0.2		301.1		
$4p_{1/2}$-$4d_{3/2}$	434.1 ± 0.05	435 [b]	439.5	440 [c]	
$4p_{3/2}$-$4d_{5/2}$	450.7 ± 0.05	450 [b]	455.9	455 [c]	
$4p_{3/2}$-$4d_{3/2}$	453.3 ± 0.1	453 [b]	458.6	457 [c]	
$4d_{3/2}$-$4f_{5/2}$	530.0 ± 0.1		536.1		
$4d_{5/2}$-$4f_{7/2}$	533.8 ± 0.05		539.9		
$4d_{5/2}$-$5p_{3/2}$	571.2 ± 0.05		578.7		
$4d_{3/2}$-$5p_{1/2}$	579.3 ± 0.05		586.8		
$4f$-$5g$	583.2 ± 0.1		596.5		
$4s_{1/2}$-$4p_{3/2}$	651.6 ± 0.1	651.57 ± 0.03 [d]	657.0	658 [c]	659 [e]
$4s_{1/2}$-$4p_{1/2}$	695.9 ± 0.1	695.91 ± 0.03 [d]	700.7	699 [c]	700 [e]
$5p_{1/2}$-$5d_{3/2}$	1059.3 ± 0.2		1067.1		
$5p_{3/2}$-$5d_{5/2}$	1096.7 ± 0.1		1103.7		
$5g$-$6h$	1157.2 ± 0.1		1162.7		
$5d_{3/2}$-$5f_{5/2}$	1191.6 ± 0.1		1203.2		
$5d_{5/2}$-$5f_{5/2,7/2}$	1199.5 ± 0.1		1211.9		
$4f_{7/2}$-$5d_{5/2}$	1267.4 ± 0.1		1278.8		
$4f_{5/2}$-$5d_{3/2}$	1276.9 ± 0.1		1288.9		
$5s_{1/2}$-$5p_{1/2}$	1766 ± 2		1774.6		
$6h$-$7i$	1929.4 ± 0.2		1931.8 [f]		

[a] Cheng and Kim,[16] relativistic Hartree-Fock, unless indicated otherwise.
[b] Druetta and Buchet,[10] beam-foil.
[c] Weiss,[14] Hartree-Fock with relativistic corrections.
[d] Fawcett, Jones, and Wilson,[19] high-temperature plasma.
[e] Cowan,[15] Hartree-Fock with relativistic corrections.
[f] Hydrogenic value.

TABLE II. Energy levels in Kr VIII.

Level	Energy (cm^{-1}) Experiment[a]	Theory[b]
$4s_{1/2}$	0	0
$4p_{1/2}$	143 697 ± 6[c]	142 711
$4p_{3/2}$	153 475 ± 7[c]	152 210
$4d_{3/2}$	374 060 ± 25	370 249
$4d_{5/2}$	375 350 ± 25	371 536
$5s_{1/2}$	490 100 ± 100	484 310
$5p_{1/2}$	546 680 ± 30	540 661
$5p_{3/2}$	550 420 ± 30	544 340
$4f_{7/2}$	562 690 ± 30	556 745
$4f_{5/2}$	562 750 ± 35	556 786
$5d_{3/2}$	641 080 ± 35	634 374
$5d_{5/2}$	641 600 ± 30	634 944
$5f$	724 980 ± 35	717 470
$5g$	734 190 ± 45	724 403
$6h$	820 610 ± 45	810 406
$7i$	872 440 ± 45	•••
limit	1 015 800 ± 200	

[a] This work, unless indicated otherwise.
[b] Cheng and Kim,[16] relativistic Hartree-Fock.
[c] Fawcett, Jones, and Wilson,[19] high-temperature plasma.

components for most of the multiplets allow us to determine the energy splittings for the $4p$, $4d$, $4f$, $5p$, and $5d$ states. These are listed in Table III, along with the relativistic Hartree-Fock predictions of Cheng and Kim[16] and our own isoelectronic extrapolations using the Dirac-Sommerfeld screening parametrization method.[30]

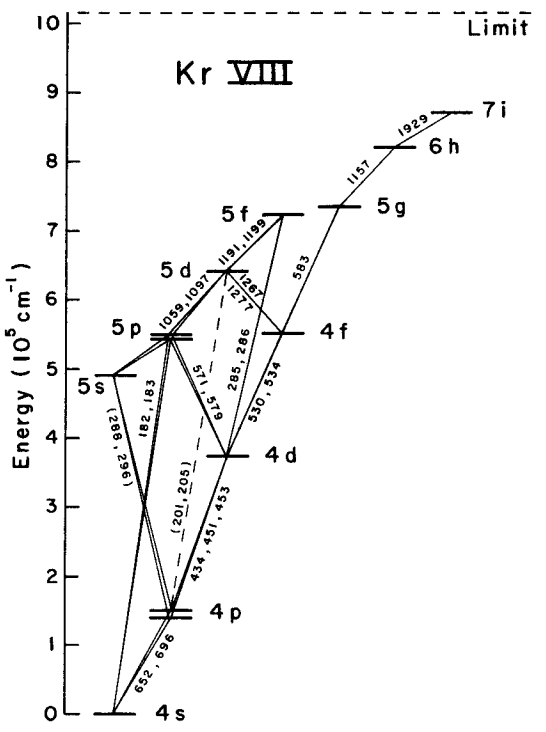

FIG. 1. Energy-level diagram for Kr VIII.

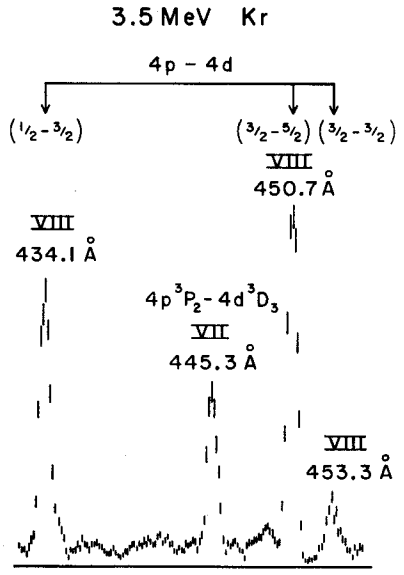

FIG. 2. Partial beam-foil spectrum of krypton, showing the $4p$-$4d$ multiplet in Kr VIII at 434.1, 450.7, and 453.3 Å and the $4s4p\,^3P_2$-$4s4d\,^3D_3$ transition in Kr VII at 445.3 Å.

B. Decays

Detailed decay curves were measured for the $4p_{1/2}$, $4p_{3/2}$, $4d_{3/2}$, $4d_{5/2}$, and $4f$ levels. About

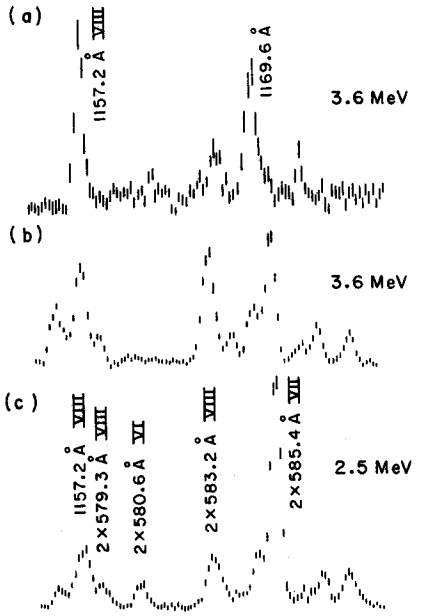

FIG. 3. The beam-foil spectrum of krypton between 1153 and 1180 Å. Spectrum (a) was measured by a detector with a LiF window, which absorbs radiation below 1050 Å. Spectra (b) and (c) were measured at different ion energies with a windowless detector to include second-order emission between 577 and 590 Å.

TABLE III. Fine-structure intervals in Kr VIII.

Levels	Interval (cm^{-1}) This work	Other experiment[a]	Theory[b]	Semiempirical[c]
$4p(\frac{1}{2}-\frac{3}{2})$	9770 ± 30	9778 ± 9	9949	9783
$5p(\frac{1}{2}-\frac{3}{2})$	3740 ± 40		3679	3783
$4d(\frac{3}{2}-\frac{5}{2})$	1290 ± 35[d]		1287	1324
$5d(\frac{3}{2}-\frac{5}{2})$	530 ± 45		569	589
$4f(\frac{5}{2}-\frac{7}{2})$	−60 ± 45		−41	

[a] Fawcett, Jones, and Wilson,[19] high-temperature plasma.
[b] Cheng and Kim,[16] relativistic Hartree-Fock.
[c] Curtis,[30] Dirac-Sommerfeld screening parametrization.
[d] This uncertainty reflects our $4p$-$4d$ wavelength uncertainty combined with the uncertainty in the $4p$ interval from Ref. 19.

ten individual decay curves were obtained for each level, and the data were summed to provide curves such as those shown in Fig. 4 for the $4p_{3/2}$ and $4d_{5/2}$ states. These data sets were then analyzed by the various fitting techniques discussed in Sec. V D.

V. ANALYSIS AND DISCUSSION

A. Spectra

The classifications listed in Table I were assigned with the aid of isoelectronic term-value interpolations, the use of a screening parameter interpolation of fine-structure separations,[30] and in particular with the guidance provided by relativistic Hartree-Fock calculations of Cheng and Kim,[16] who utilize a computer program originated by Desclaux.[31] The charge-state dependence of the variation of line intensity with ion energy was employed to confirm the Kr VIII classifications. Most lines were observed in both first and second order (occasionally in third order) for the purpose of improving the wavelength resolution and eliminating certain line-blending problems.

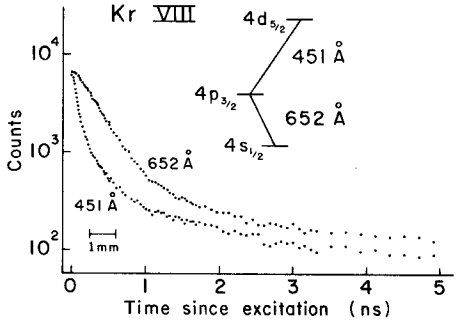

FIG. 4. Intensity decay data for the foil-excited $4p_{3/2}$ and $4d_{5/2}$ states in Kr VIII.

The spectrum of Kr VIII is strongly excited in the beam-foil source at the ion energies we used. Transitions among low-lying levels and transitions involving high l states for higher n are normally strong, so that most of our spectroscopic classifications are unambiguous. The existence of several closed loops within the level scheme for each of the two strong ($\Delta J \neq 0$) fine-structure components provides confirmation for the classifications. The $4p$-$5d$ transitions (near 200 Å) were not observed, but this is not surprising since there is an accidental cancellation in the associated transition integral[16,32] for Kr VIII, allowing the $5d$ state to deexcite almost entirely via the $5p$ and $4f$ states. This absence of cascade repopulation of $4p$ by $5d$ is important in the analysis of the decay of the $4p$ state, as will be discussed below. The Z-dependent characteristics of such cancellations have been discussed recently by Curtis and Ellis.[32] Our independent determinations of the $4p$- and $5d$-level energies predict wavelength values of 201.05 and 204.87 Å (±0.02 Å) for the $4p$-$5d$ transitions. Our classifications of the $4p$-$5s$ transitions at 288.5 ± 0.3 Å and 297.1 ± 0.2 Å and our $5p$-level determination via $4d$ are consistent with our classification of the $5s$-$5p_{1/2}$ transition at 1766 ± 2 Å. The $5s$-$5p_{3/2}$ transition should then appear at 1657 ± 2 Å and is probably masked in our spectra by a strong neutral carbon multiplet emitted by excited atoms sputtered from the foil.

Comparison of our observed level scheme with that predicted by relativistic Hartree-Fock calculations[16] for Kr VIII indicates that the theoretical excitation energies (relative to $4s$) are uniformly about 1.0% too low for all the levels observed. If we scale the theoretical energies by this empirical correction factor, the agreement between the theoretical values[16] and our results becomes better

than 0.1% for the $4d$, $4f$, $5p$, $5d$, and $5f$ states, whereas the theoretical $5s$-, $5g$-, and $6h$-level energies remain about 0.2% too high and those of the $4p$ levels lie about the same amount too low. It is interesting to note that qualitatively similar trends are revealed by comparison of the results of Ref. 16 with recent measurements of the spectra of copperlike Se VI [5] and Mo XIV, [6] suggesting the presence of at least an l-dependent effect that is not accounted for in the calculations.

Our wavelength results show that the $4f$ state in Kr VIII possesses inverted fine structure (see Table III), in agreement with the relativistic Hartree-Fock values.[16] The results of Ref. 16 reflect the difference in the interactions between the core and valence electrons for $4f_{5/2}$ and $4f_{7/2}$, within the Hartree-Fock approximation, that are included in these relativistic calculations. Our observations are consistent with the anomalously small, but positive, $4f$ splitting observed by Reader *et al.*[6] in copperlike Mo XIV. Similar inversions or distortions of fine-structure intervals have been known for some time in certain series of excited states in alkali-metal atoms.[33] These fine-structure anomalies are attributed to the effects of configuration interaction with core-excited inverted doublet terms lying above the series limit,[33,34] and they have been the subject of recent calculations.[35]

Finally, we point out that the wavelength values reported previously by Druetta and Buchet[10] for the $4p$-$4d$ multiplet in Kr VIII are inaccurate by ~1 Å. Furthermore, the tentative classifications suggested and tabulated previously by Kelly and Palumbo[36] for the transitions $4p$-$5s$, $4p$-$4d$, and $4p$-$5d$ are incorrect.

B. Ionization potential

Since no more than two members of any Rydberg series have been established for this ion, it was not possible to determine the ionization potential through Ritz expansions of the quantum defects. However, the energies relative to the ground state for five "nonpenetrating" levels were measured in the experiment, so it was possible to determine the ionization potential from a screened hydrogenic model with core polarization. For nonpenetrating orbits (i.e., l greater than the value of any core electron) the energy $E(n,l)$ relative to the ground state (neglecting fine structure) can be written[37]

$$E(n,l) = I_0 - T_H(n,l) - \alpha_d \langle r^{-4} \rangle_{nl} - \alpha_q \langle r^{-6} \rangle_{nl} , \qquad (8)$$

where I_0 is the ionization potential, $T_H(n,l)$ and $\langle r^k \rangle_{nl}$ are the Sommerfeld term value and expectation value of r^k for a hydrogenic system of effective charge given by the atomic number minus the number of core electrons, and α_d and α_q are the effective electric dipole and electric quadrupole polarizabilities of the core. The units of $E(n,l)$ are Rydbergs; the units of r are a_0 and the units α_d and α_q are a_0^3 and a_0^5, respectively, where a_0 is the Bohr radius. Formulas for T_H, $\langle r^{-4} \rangle_{nl}$, and $\langle r^{-6} \rangle_{nl}$ are given in Refs. 34 and 37. Since I_0, α_d, and α_q are constants for a given ion, they can be determined from Eq. (8) if three or more $E(n,l)$ values are known.

The $4f$, $5f$, $5g$, $6h$, and $7i$ levels are all nonpenetrating and have been measured. However, the $4f$ level has inverted fine structure, and the ^2F series may be influenced by perturbations which cause it to deviate from the hydrogenic model of Eq. (8). A similar inversion of the fine structure is observed for the $3d$ state of the sodium isoelectric sequence,[34] and there Eq. (8) is valid only for $l \geq 3$ despite the nonpenetrating nature of the ^2D series. For the sodium sequence, the perturbations of the ^2D series have been described in terms of configuration interaction with ^2D terms produced by the excitation of the $2p^6$ shell, and a similar argument could be made for the perturbation of the ^2F series in the copper sequence owing to configuration interaction with ^2F terms produced by excitation of the $3d^{10}$ core. We have therefore determined the ionization potential variously including none, either, and both of the ^2F energy values. For the $4f$ level, the centroid of the multiplet was used in the calculations. Least-squares fits were made, and the resulting parameters and the value of chi-squared per degree of freedon (d.f.) for each fit are given in Table IV. Clearly the number of ^2F levels included in the fit has a considerable effect on the determination of polarizability parameters, but the ionization potential inferred is quite insensitive to the levels included. Making generous allowance for possible uncertainties, we have adopted the value $I_0 = 1\,015\,800 \pm 200$ cm^{-1}. This corresponds to $125.94 \pm .02$ eV, and is in agreement with, but of higher precision than a number of theoretical calculations, which have yielded 126, 123, 125.4, 124, 125, and 123 eV (from Refs. 38, 39, 15, 13, 40, and 40, respectively), but disagrees with a calculation[41] of 133.3 eV. The

TABLE IV. Least-squares fits to the polarization formula for Kr VIII.

Levels included	I_0 (cm^{-1})	α_d	α_q	χ^2/d.f.
$4f$, $5f$, $5g$, $6h$, $7i$	1 015 864	0.156	0.516	1.9
$4f$, $5g$, $6h$, $7i$	1 015 815	0.093	0.562	0.012
$5f$, $5g$, $6h$, $7i$	1 015 816	0.100	0.544	0.016
$5g$, $6h$, $7i$	1 015 823	0.132	0.456	•••

values for α_d and α_q are only crudely determined, but clearly indicate the importance of the quadrupole polarizability. Using these values together with Table IX of Ref. 34, one can see that $\alpha_q\langle r^{-6}\rangle_{nl}$ dominates over $\alpha_d\langle r^{-4}\rangle_{nl}$ for the ^2F and ^2G series in Kr VIII, and is a large fraction of the total polarization energy for the ^2H and ^2I series.

We note that the precision of our derived value for the ionization potential in Kr VIII is higher than that reported recently[6] for the isoelectronic ion Mo XIV, from high-resolution spectroscopy of a laser-produced plasma. This is possible because of the efficiency of the beam-foil source for the production of high-l (yrast) states, which are less susceptible to perturbations than are the lower-l states produced in the plasma source.

C. Simulated decay curves

A computer simulation of the $4s-4p$ decay curves for Kr VIII, using a population model $(2l+1)\,(n^*)^{-p}$ with $p=2-5$, and an instrumental resolution of 30 ps, is shown in Fig. 5. Here the dashed line represents the mean life to be extracted, and the solid circles represent our measured data. For $n^*\cong n$ and $p>3$ this population model can be summed over infinite n and $l\leq n-1$, to obtain a finite normalization in terms of the Riemann ζ function, whereas for $p\leq 3$ this sum is divergent. Simulated decay curves using normalizable population models have been studied by Crossley *et al.*[21] They found, as can be seen here from Fig. 5, that long-lived decay tails are not produced for the higher ionization stages when such a normalizable population model is assumed, and that lifetimes should be reliably extractable. Younger and Wiese[22] have simulated decay curves for the $4p$ state in copperlike ions, using this type of model with $p=3$ truncated at a maximum value of n, and found that this can lead to long-lived decay tails. They conclude that, in such cases, reliable extraction of mean lives would be difficult by standard curve-fitting procedures. The experimental situation regarding the appropriate population model to be used is not clear at present. In some cases long tails, which can only be explained in terms of bound-state cascades through the inclusion of a very heavy population of states of very high n, are indeed observed. For example, Pegg *et al.*[42] have reported very strong tails in the lowest $^2P_{3/2}$ resonance transition of Cu XIX in the Na I sequence. Forester *et al.*[43] have studied Cl IX–Cl XV and found that such tails occur for N-, O-, and F-like Cl but not for the lines studied in C-like or more highly stripped Cl ions. It can be seen in Fig. 5 that the decay curves measured in this experiment also contain tails which cannot be explained by cascades from levels populated according to the distribution $(2l+1)\,(n^*)^{-p}$, with p greater than the limiting value for normalizable populations.

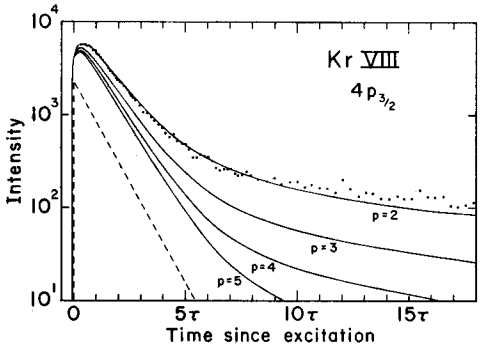

FIG. 5. Computer simulations of the intensity decay curve for the foil-excited $4p_{3/2}$ state in Kr VIII. The population model $(2l+1)(n^*)^{-p}$ was applied, for $p=2$, 3, 4, and 5. Theoretical lifetimes for the $5s$, $5p$, $6s$, and $6p$ levels and the yrast ($l=n-1$) chain up to $n=26$ were included. A rectangular instrumental resolution function 30-ps wide has also been convoluted with the decay curve. The points represent measured data.

D. Lifetimes

1. *Joint analysis of decays*

The experimental decay curves contained 90 channels with a common origin relative to the foil position for all measurements. Channel 5 was determined to be the first point at which effects of upstream viewing and vignetting of the foil have completely vanished. For purposes of applying Eq. (6) the channels were grouped into sets [denoted henceforth as "panels" after Ref. (44)] of 3, 5, or 7 channels each. The effective values for the decay curves and the $4p$ logarithmic derivative were computed by fitting data points within each panel to a polynomial in the logarithm, and evaluating the central magnitude and slope. The panels were nonoverlapping, i.e., the data contained in each panel were independent of those in the other panels. We performed panel polynomial fits for $4p$ by two alternative methods: using all data in each panel to compute both the central intensity and its derivative, and dividing the data into two subsets, using one to compute the central intensity and the other to compute its derivative. With the former method there is correlation between the uncertainties in x and y [Eqs. (3) and (4)], which is avoided in the latter method. With both methods the uncertainties were treated as if they were uncorrelated, and each panel was assigned a weight based upon an incoherent sum of the statistical uncertainties propagated into x and y [cf. Eq. (3.57) of Ref. 23]. The values and un-

certainties inferred for τ_{4p} by these two methods did not significantly differ, and we conclude that the correlations between uncertainties in x and y can, at least in this case, be neglected. A plot of $d(\ln I_{4p})/dt$ vs I_{4d}/I_{4p} is shown in Fig. 6.

Contributions to x_0 from $5s_{1/2}$ were included in an extended analysis, but because the measured decay curve for $5s_{1/2}$ diminished rapidly to zero, the results were virtually indistinguishable from those of Fig. 6. The degree to which the experimentally determined variables y and x conform to a straight-line dependence confirms that x_0 is indeed negligible for this case, and that all significant cascade effects in the $4p_{3/2}$ decay curve are included in the $4d_{5/2}$ decay curve. Purely statistical uncertainties were approximately one percent. However, a somewhat larger uncertainty in the derived mean life arises from the sensitivity of this value to the details of the grouping of points in the derivative computation and to the number of data points included in the fitting procedure. The $4p_{3/2}$-state lifetime that results from this analysis is 243 ±10 ps.

We attempted similar analyses for the $4p_{1/2}$ state, using decay data for 696 and 434 Å. However, the results were generally poor, with nonlinear plots of Eq. (6) and large scatter in the fits suggesting the absence of complete correlation between the two data sets. We suspected the cause to be our inability to spectroscopically resolve the KrVII $4p\,^3P_1$-$4d\,^3D_2$ line at 434.28 Å from the KrVIII $4p_{1/2}$-$4d_{3/2}$ line at 434.1 Å, as discussed in Sec. IV A. This was confirmed by our joint analysis of 696 Å with 450 Å, which yielded good fits and a value of 291 ± 12 ps for the $4p_{1/2}$ lifetime. This latter analysis is not strictly correct, since 450 Å represents the cascade into $4p_{3/2}$ instead of $4p_{1/2}$, but the decay characteristics of $4d_{3/2}$ and $4d_{5/2}$ are not expected to be substantially different. We note also that the cube of the p-state lifetime ratio is identical to the ratio of $4s$-$4p$ transition wavelengths, as expected theoretically under pure LS-coupling conditions. Oscillator strengths derived from these $4p$-state lifetimes will be compared in Sec. V D 3 with previous measurements and with theory.

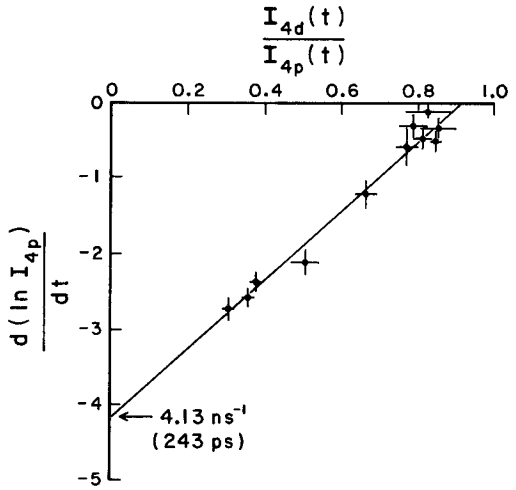

FIG. 6. Plot of the combined $4p_{3/2}$, $4d_{5/2}$ decay data according to the variables of Eq. (6). The intercept of the fitted line with the y axis determines the reciprocal lifetime of the $4p_{3/2}$ level. The good fit indicates that all significant cascades pass through the $4d_{5/2}$ level.

Decay data for the unresolved $4f$ states measured at 534 Å were also analyzed in conjunction with the decay data for the $4d$ states. Attempts at carrying out a correlated analysis for the 534-434 Å pair showed that these data were not described by a linear form analogous to Eq. (6), again reflecting the line blending occurring at 434 Å. On the other hand, the 534-450 Å pair gave a good fit and yielded a lifetime value of 48 ±4 ps for the $4d_{5/2}$ state. This result compares favorably with the $4d_{5/2}$ lifetime value of 50 ps from the relativistic Hartree-Fock calculations of Cheng and Kim[16] and of Wiess[14] and with the value of 51 ps from the Coulomb approximation results of Lindgård *et al.*,[18] but less well with the Hartree-Fock $4d$-state multiplet value of 64 ps from Younger and Wiese.[22]

2. *Multiexponential fitting*

The decay data for the $4p_{1/2}$ and $4p_{3/2}$ states were also analyzed by multiexponential least-squares fits in order to ascertain under what circumstances reasonable mean lives can be obtained by this technique. If unconstrained two-exponential fits are performed, apparent mean lives of 390 and 330 ps are found for the $4p_{1/2}$ and $4p_{3/2}$ states, respectively—in essential agreement with the previous measurements of Refs. 10–12. This verified the Younger and Wiese[22] suggestion that in this instance a simple two-exponential fit is likely to give erroneous results. The situation can be improved, however, by performing *constrained* multiexponential fits based upon insight into the nature of the decay scheme being studied. Two physically significant aspects are immediately recognized: (a) there are likely to be cascade effects from shorter-lived levels ($\tau \cong 50$, 170 ps) which cause the observed "growing-in" of the measured decay curves and which require negative-amplitude mean life components in a multiexponential fit, and (b) it is possible that cascading along the yrast chain will introduce one mean life component in the observed decay curve (the 330 ps meanlife of the $7i$ level) which is close enough in value to the meanlife of the $4p$ level to distort an unconstrained exponential analysis. (Mean lives

of such high-lying members of the yrast chain as this level are relatively well described by the hydrogenic values assumed in this argument.)

A simple test for the presence of short-lived cascades may be carried out by performing successive two-exponential fits to decays from which additional initial data points have been removed. A significant decrease in the fitted shorter lifetime normally indicates a growing-in decay curve. For both the $4p_{1/2}$ and $4p_{3/2}$ decays, we observed a substantial reduction of lifetime resulting from the exponential fits as well as a decrease in the reduced χ^2 as data points were eliminated, indicating that the inclusion of one or more fast negative decay components in the curve fits was clearly necessary.

Constrained multiexponential fits were therefore carried out, which required the presence of one or two negative-amplitude decay contributions, and possibly one fixed 330-ps lifetime contribution. In Fig. 7 we have plotted the $4p$ lifetimes that result from three- through nine-exponential fits to our decay data, incorporating either one or two negative components. (The two-exponential unconstrained fit results are included for comparison.) In no case during these fits would the data allow more than two unconstrained positive exponential components to remain distinct in value. Thus, in order to achieve fits with five or more exponentials, one or more long-lived cascade components were constrained to hydrogenic lifetime values for $n \geq 7$, these being expected to dominate among possible cascade contributions. The results shown in Fig. 7 reveal the importance of including both of the expected growing-in cascade contributions in the fits (especially for $4p_{1/2}$). When this is done the results display essentially no dependence upon the number of decay components fitted. In particular, there was little effect on the $4p$ lifetime when the expected 330-ps cascade component was not constrained in value. The effects of the growing-in components were the predominant features of the multiexponential analysis. Since the reduced-χ^2 values obtained were also nearly independent of the number of fit parameters, we have chosen in each case the approximate mean values of the various fits involving the growing-in cascades, namely 300 ±25 and 270 ±20 ps, to represent the constrained multiexponential fit lifetimes for the $4p_{1/2}$ and $4p_{3/2}$ levels, respectively. The uncertainties quoted here represent simply the maximum spreads in these results, as an attempt to approximate systematic errors (due to cascade contributions) that are much larger than the statistical errors of the individual fits.

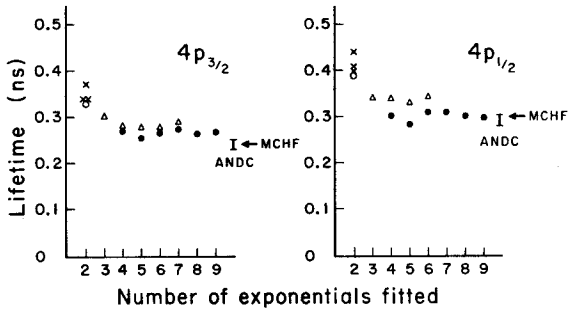

FIG. 7. Lifetime results for the $4p_{1/2}$ and $4p_{3/2}$ states obtained by multiexponential fitting of the decay data for the individual levels. Results are shown for two to nine fitted exponential components, including zero(○), one(△), or two(●) short-lived (growing-in) cascades. For comparison our correlated-decay (ANDC) results are indicated, as are the lifetimes derived from the multiconfiguration Hartree-Fock calculation of Froese Fischer (Ref. 13).

3. *Comparison with other results*

In Table V we have summarized our lifetime results for the $4p$ states, as well as results obtained by previous investigations, in terms of absorption oscillator strengths (f values) that are derived directly from the lifetimes. These experimental results are compared with various theoretical f values, also shown in Table V. The non-

TABLE V. f values for $4s$-$4p$ in Kr VIII.

$4s_{1/2}$-$4p_{1/2}$	$4s_{1/2}$-$4p_{3/2}$	Reference (experiment)
0.25 ± 0.01	0.53 ± 0.02	This work[a]
0.24 ± 0.02	0.47 ± 0.04	This work[b]
0.25 ± 0.01	0.59 ± 0.09	Pinnington *et al.*[c]
0.18 ± 0.01	0.39 ± 0.01	Irwin *et al.*[d]
0.18 ± 0.02	0.39 ± 0.03	Druetta and Buchet[d]
0.16 ± 0.02	0.34 ± 0.05	Knystautas and Drouin[d]
		(Theory)
0.246	0.526	Froese Fischer[e]
0.278	0.597	Cheng and Kim[f]
0.278	0.600	Weiss[g]
0.28	0.59	Cowan[g]
0.261	0.563	Lindgård[h]
0.220	0.473	Migdalek and Baylis[i]

[a] Jointly analyzed decay curves.
[b] Multiexponential fits.
[c] New beam-foil measurement.[45]
[d] Previous beam-foil measurement.[10-12]
[e] Multiconfiguration Hartree-Fock.[13]
[f] Relativistic Hartree-Fock.[16]
[g] Hartree-Fock with relativistic corrections.[14,15]
[h] Coulomb approximation.[18]
[i] Model potential.[17]

relativistic multiconfiguration Hartree-Fock calculation of Froese Fischer[13] provides only a multiplet f value (0.772). However, the fine-structure f values may be derived by assuming the individual $4s$-$4p$ line strengths are equal and simply scaling the f-value components in proportion to their transition wavelengths. These values are given in Table V. In addition, we note that all the nonrelativistic results of Ref. 13 quoted in Table V have been multiplied by the factor 1.044 to reflect the fact that experimental transition energies were not used in those calculations.

The lifetime results from our correlated-decay analysis and those from our constrained multiexponential fitting agree fairly well with each other, although the former results are more fundamentally valid and are expected to be more reliable, as discussed above. We have therefore based our experimental estimates for the $4p$ lifetimes and their uncertainties entirely on the correlated-decay analysis. Previous beam-foil results by curve-fitting methods are seen to have yielded f values that are about 30% lower than our values. Our multiexponential-fitting analysis suggests that the previously reported lifetime values are too long, owing in part to the failure of earlier investigators to recognize the characteristics of the atomic structure of copperlike systems and consequently to allow for adequate cascade contributions (in particular from shorter-lived levels) in the fitting of the decay data. Our correlated-decay analysis has provided reliable lifetimes for the $4p$ levels in Kr VIII and has enabled us to appraise the reliability of the multiexponential-fitting method when it is partially constrained to reflect the characteristics of the excited-state structure.

Our correlated-decay results are in excellent agreement with the multiconfiguration Hartree-Fock (MCHF) values of Froese Fischer.[13] Since electron correlation effects dominate over relativistic corrections for these f values in Kr VIII, we expect these MCHF values to be the most reliable of the theoretical results listed in Table V. Comparison of the results of Ref. 13 with the results of relativistic calculations suggests that the electron correlation effects produce a reduction in f value by about 15%. A very recent model-potential approach[17] to the treatment of core polarization yields even lower f values.

VI. CONCLUSION

Our study of the beam-foil spectrum of krypton has enabled us to greatly extend the known excited-state structure of Kr VIII and to provide the first extensive comparison between experiment and recent relativistic atomic structure calculations for moderately ionized copperlike systems. Our measurement and detailed analysis of the $4p$-state lifetime in Kr VIII have eliminated the previous discrepancy between experiment and theory for this value and have helped clarify the extent to which certain cascade effects contribute to observed beam-foil decays.

Our present $4p$-state lifetime measurement confirms recent suspicions that strong cascade contributions in the observed decay of this state, coupled with incomplete analysis of the earlier data, were the dominant source of previous discrepancies between theory and experiment. We have shown here that by a joint analysis of correlated-decay curves the cascade contributions can be accurately accounted for and reliable lifetimes obtained. At the same time, we point out that the multiexponential-fitting analysis of complicated decay data may be greatly improved by utilizing known aspects of the excited-state decay scheme and may also yield reliable, although less precise, lifetimes. We suggest that the careful application of both analysis techniques in a complementary fashion can be used to provide reliable experimental lifetime results in the future.

The atomic structure results presented here for Kr VIII affirm the utility of beam-foil spectroscopy, with its inherently modest resolution, in providing guidance for advanced atomic calculations of even single-valence-electron heavy ions. For more complicated valence-shell structures, where electron correlation effects further decrease theoretical accuracy, this spectroscopic source will prove to be of equal or greater value in the determination of atomic structures for lower as well as much higher degrees of ionization.

Note: An independent study of the $4p$ lifetime in Kr VIII using correlated-decay analysis techniques has been reported by Pinnington *et al.*[45] Their results have been included in Table V.

Note added in proof. It has been pointed out to us by J. Reader that isoelectronic interpolation using his unpublished data [see J. Opt. Soc. Am. 69, 1285 (1979)] for heavier ions suggests that the $4f$-$5g$ transition in Kr VIII lies near 585.6 Å instead of 583.2 Å. This transition would then be blended with the strong resonance line of Kr VII in our spectra (see Fig. 3). Although we cannot rule out this possibility, we would then be unable to classify the strong line in our spectra at 583.2 Å, which appears to belong to the spectrum of Kr VIII or IX. If the $4f$-$5g$ transition occurs at 585.6 Å, our derived value for the ionization potential of Kr VIII becomes $1\,015\,100 \pm 200$ cm^{-1}, and our derived electric dipole and quadrupole polarizabilities are not significantly affected.

ACKNOWLEDGMENTS

We wish to thank K. T. Cheng and Y-K. Kim for providing us with Dirac-Hartree-Fock results of energies and transition probabilities for copper-like ions in advance of publication, and we are pleased to acknowledge numerous fruitful discussions with K. T. Cheng regarding the copper isoelectronic sequence. We also thank B. L. Cardon and J. A. Leavitt for providing us with their wavelength list from the beam-foil spectrum of krypton in advance of publication. We are grateful to J. Reader for helpful advice on the 5*s*-level classification in Kr VIII and for pointing out the possible difficulty concerning the wavelength of the $4f$-$5g$ transition. This work was supported in part by the U. S. DOE Basic Energy Division of Chemical Sciences.

---

*Present address: Dept. of Physics, Univ. of Notre Dame, Notre Dame, Ind. 46556.
†Dept. of Physics and Astronomy, Univ. of Toledo, Toledo, 43606.

[1]E. Hinnov, Phys. Rev. A 14, 1533 (1976).
[2]E. Alexander, M. Even-Zohar, B. S. Fraenkel, and S. Goldsmith, J. Opt. Soc. Am. 61, 508 (1971).
[3]J. Reader and N. Acquista, Phys. Rev. Lett. 39, 184 (1977).
[4]L. J. Curtis, A. Lindgård, B. Edlén, I. Martinson, and S. E. Nielsen, Phys. Scr. 16, 72 (1977).
[5]Y. N. Joshi and Th. A. M. van Kleef, Physica 94C, 270 (1978).
[6]J. Reader, G. Luther, and N. Acquista, J. Opt. Soc. Am. 69, 144 (1979).
[7]M. W. D. Mansfield, N. J. Peacock, C. C. Smith, M. G. Hobby, and R. D. Cowan, J. Phys. B 11, 1521 (1978).
[8]T. Anderson and G. Sørensen, Phys. Rev. A 5, 2447 (1972); G. Sørenson, *ibid.* 7, 85 (1973).
[9]E. H. Pinnington, J. A. Kernahan, and K. E. Donnelly, J. Opt. Soc. Am. 67, 162 (1977).
[10]M. Druetta and J. P. Buchet, J. Opt. Soc. Am. 66, 433 (1976).
[11]D. J. G. Irwin, J. A. Kernahan, E. H. Pinnington, and A. E. Livingston, J. Opt. Soc. Am. 66, 1396 (1976).
[12]E. J. Knystautas and R. Drouin, J. Quant. Spectrosc. Radiat. Transfer 17, 551 (1977).
[13]C. Froese Fischer, J. Phys. B 10, 1241 (1977).
[14]A. Weiss, J. Quant. Spectrosc. Radiat. Transfer 18, 481 (1977).
[15]R. D. Cowan, Los Alamos Report No. LA-6679-MS (National Technical Information Service, Springfield, Va., 1977).
[16]K. T. Cheng and Y-K. Kim, At. Data Nucl. Data Tables 22, 547 (1978).
[17]J. Migdałek and W. E. Baylis, J. Phys. B 11, L497 (1978); 12, 1113 (1979).
[18]A. Lindgård, L. J. Curtis, I. Martinson, and S. E. Nielson, Phys. Scr. (to be published).
[19]B. C. Fawcett, B. B. Jones, and R. Wilson, Proc. Phys. Soc. London 78, 1223 (1961).
[20]B. Cardon, Ph.D. thesis, University of Arizona, 1977 (unpublished).
[21]R. J. S. Crossley, L. J. Curtis, and C. Froese Fischer, Phys. Lett. A 57, 220 (1976).
[22]S. M. Younger and W. L. Wiese, Phys. Rev. A 17, 1944, (1978); 17, 2366 (1978).
[23]A review and bibliography of these lifetime analysis methods has been given by L. J. Curtis in *Beam Foil Spectroscopy*, edited by S. Bashkin (Springer-Verlag, Berlin, 1976), Chap. 3, pp. 63–109. See also L. J. Curtis, J. Phys. (Paris) 40, C1–139 (1979).
[24]J. Lindhard, M. Scharff, and N. E. Schiøtt, K. Dan. Vidensk. Selsk. Mat. Fys. Medd. 33 (14) (1963).
[25]J. O. Stoner, Jr., and J. A. Leavitt, Appl. Phys. Lett. 18, 477 (1971).
[26]B. Edlén, Phys. Scr. 11, 366 (1975).
[27]L. Barrette and R. Drouin, Phys. Scr. 10, 213 (1974); H. G. Berry, J. Désesquelles, P. Tryon, P. Schnur, and G. Gabrielse, Phys. Rev. A 14, 1457 (1976).
[28]E. Schönheit, Optik (Stuttgart) 23, 409 (1966).
[29]A. E. Livingston, J. Phys. B 9, L215 (1976).
[30]L. J. Curtis, Phys. Lett. A 64, 43 (1977); *ibid.* 72, 427 (1979).
[31]J. P. Desclaux, Comput. Phys. Commun. 9, 31 (1975).
[32]L. J. Curtis and D. G. Ellis, J. Phys. B 11, L543 (1978).
[33]H. E. White, *Introduction to Atomic Spectra* (McGraw-Hill, New York, 1934), p. 393.
[34]B. Edlén, Phys. Scr. 17, 565 (1978).
[35]R. M. Sternheimer, J. E. Rodgers, and T. P. Das, Phys. Rev. A 17, 505 (1978).
[36]R. L. Kelly and L. J. Palumbo, Naval Research Lab Report No. 7599 (1973) (unpublished).
[37]B. Edlén, in *Handbuch der Physik* (Springer, Berlin, 1964), Vol. XXVII, p. 80.
[38]W. Finkelnburg and W. Humbach, Naturwissenschaften 42, 35 (1955).
[39]R. L. Kelly and D. E. Harrison, Jr., At. Data 3, 177 (1971).
[40]S. Fraga, J. Karwowski, and K. M. S. Saxena, *Handbook of Atomic Data* (Elsevier, New York, 1976), p. IV(3)-9.
[41]T. A. Carlson, C. W. Nestor, Jr., N. Wasserman, and J. D. McDowell, At. Data 2, 63 (1970).
[42]D. J. Pegg, P. M.Griffin, B. M. Johnson, K. W. Jones, J. L. Cecchi, and T. H. Kruse, Phys. Rev. A 16, 2008 (1977).
[43]J. P. Forester, D. J. Pegg, P. M. Griffin, G. D. Alton, S. B. Elston, H. C. Hayden, R. S. Thoe, C. R. Vane, and J. J. Wright, Phys. Rev. A 18, 1476 (1978).
[44]E. H. Pinnington and R. N. Gosselin, J. Phys. (Paris) 40, C1–149 (1979).
[45]E. H. Pinnington, R. N. Gosselin, J.A. O'Neill, J. A. Kernahan, K. E. Donnelly, and R. L. Brooks, Phys. Scr. 20, 151 (1979).